

# Modeling Retinal Waves in Starburst Amacrine Cells



Ben Lansdell\*,†, J. Nathan Kutz† and Kevin Ford‡

† Department of Applied Mathematics, University of Washington

‡ University of California San Francisco

\*lansdell@uw.edu

## Introduction

Retinal waves are examples of spontaneous correlated activity in the developing central nervous system, and are believed to play a role in the refinement of retinal projections. This activity occurs in developing neural circuits prior to visual stimulus. The waves are the result of neighboring retinal cells spiking in a coordinated fashion which can spread across the entire retina. Here we study the transient cholinergic network which exists in the starburst amacrine cell (SAC) layer in rodents in post-natal days 1-10 (so called stage II waves). [1]

## Aims

- Develop simple mathematical framework capable of recapitulating dynamics of retinal waves
- Investigate role of cell intrinsic noise and cell-cell variability in wave properties
- Bifurcation analysis: determine parameter regimes capable of supporting traveling wave solutions

## Mathematical framework

In contrast to previous models of retinal waves (see [2] for a review), following the suggestion in [3] that retinal waves are mediated by extrasynaptic transmission of acetylcholine, our model takes the form of a reaction-diffusion system:

$$\begin{aligned} V_t &= f(V, R, E) \\ R_t &= \varepsilon g(V, R, E) \\ E_t &= h(V, R, E) + \varepsilon^2 \nabla^2 E \end{aligned}$$

(dimensionless)  
 $V$ : fast voltage variable  
 $R$ : slow 'refractory' variable  
 $E$ : ACh concentration  
 $0 < \varepsilon \ll 1$ : separation of time scales

To facilitate mathematical analysis, build heuristic model based on Fitzhugh-Nagumo (FN) neuron dynamics, with the following choice of  $f, g$  and  $h$ :

$$\begin{aligned} f(V, R, E) &= V(1 - V)(V - A) + E - R \\ g(V, R, E) &= BV - CR \\ h(V, R, E) &= \beta G(V) - \gamma E. \end{aligned}$$

where

$$G(V) = \frac{1}{1 + \exp[-\kappa(V - V_0)]},$$

$$0 < A < 1,$$

$$B, C, \beta, \gamma > 0.$$

## Deterministic models

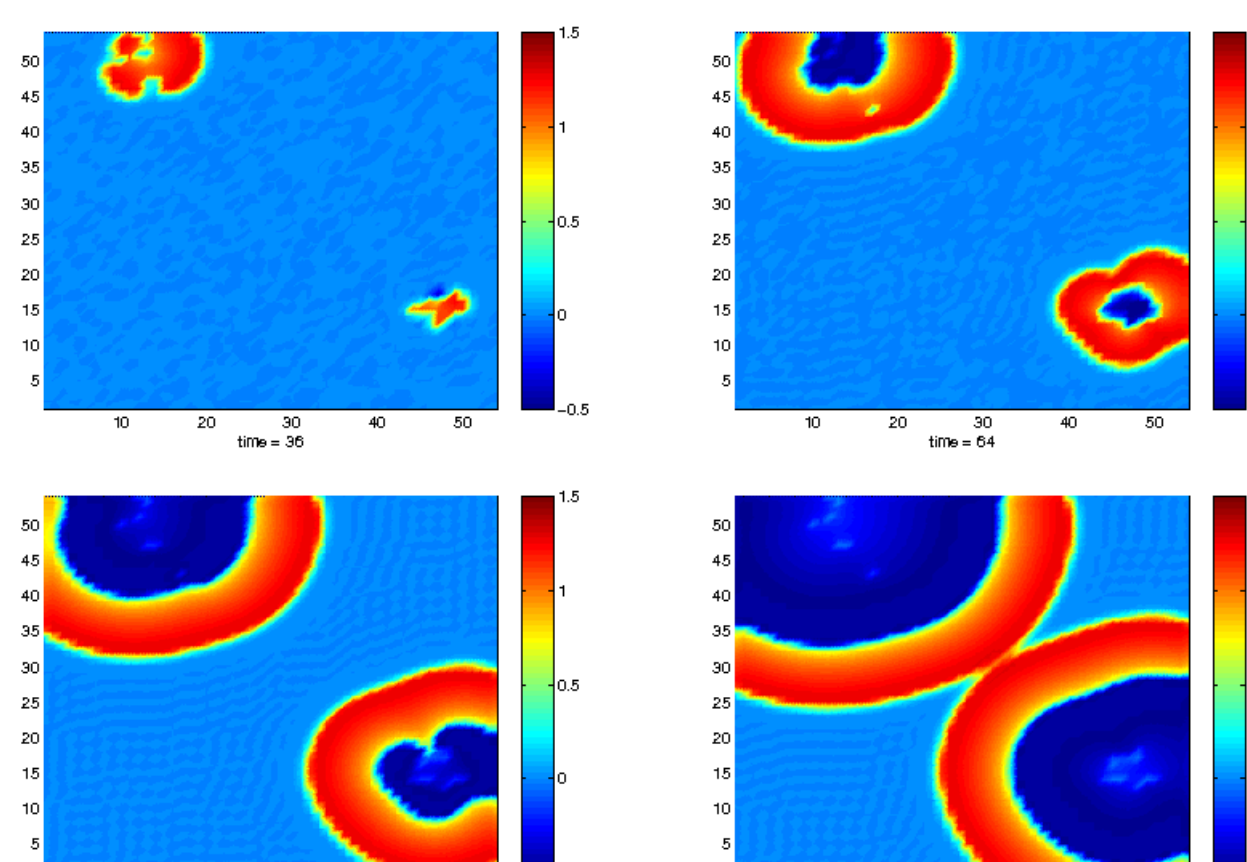


**Figure 1:** Wave formation shown at successive times. Here  $A = 0.2, B = 0.2, C = 0.0001, \varepsilon = 0.1, \beta = 0.4, \gamma = 0.7, \kappa = 100, V_0 = 0.3$ . Color represents voltage.

Deterministic simulations produce waves (Figure 1) but exhibit two unrealistic qualities:

1. Once a wave is initiated it covers entire domain: stage II waves are known to exhibit power-law size distributions.
2. A strong tendency to generate spiral waves: the FN model does not encompass a sAHP current present in SACs which generates long refractory periods.  
 $\Rightarrow$  The shifting boundaries and power-law distributed sizes and speeds of retinal waves need (a) cell-intrinsic noise or cell-cell variability and (b) a long, spike-size dependent refractory period in order to desynchronize the waves and prevent spirals.

Before turning to stochastic models the wave properties of the deterministic model are studied. We use asymptotic and numerical continuation methods to study our FN equations in one spatial dimension.

## Singular construction of traveling pulse

By extending the analysis outlined in [4], scaling variables appropriately and setting  $\varepsilon = 0$  the inner and outer systems are obtained:

### Inner system

In regions where diffusion is large, let  $\tau = t, \xi = (x - c(R)t)/\varepsilon$ , to give

$$\begin{aligned} -cV' &= f(V, R, E) \\ -cR' &= 0 \\ -cE' &= h(V, R, E) + E'', \end{aligned}$$

where  $' = \partial/\partial\xi$ . At a fixed refractory variable  $R$ , wave speed  $c(R)$  is computed by finding heteroclinic orbits connecting rest state to excited state. This provides a threshold refractoriness  $R^*|c(R^*) = 0$  for regions above which, waves cannot propagate into. Singular construction of a traveling pulse is possible if there exists  $R^*$  such that the speed of the up-jump is exactly opposite the speed of the down-jump:  $c(0) = -c(R^*)$ . (Figure 2)

### Outer system

In between up- and down- jumps dynamics are given by a one dimensional system (original scaling):

$$R' = G_{\pm}(R),$$

where  $' = d/dt$ ,  $G_+$  and  $G_-$  are excited and recovery branches. This provides estimates for the interwave-interval and wave duration by computing time spent in excited and recovery states (on  $G_+$  and  $G_-$  branches):

$$t_{ex} = \int_{R_0}^{R_+} \frac{dR}{G_+(R)}, \quad t_{rec} = \int_{R_+}^{R^*} \frac{dR}{G_-(R)}.$$

where  
 $R_0$  = rest value,  
 $R_+$  = excited value at down-jump,  
 $R^*$  = end of recovery value.

## Non-singular construction of traveling pulse

Beyond the singular limit, the entire pulse can be studied by switching to a traveling frame  $(x, t) \rightarrow (x - ct, t)$  and looking for stationary solutions ( $V_t = 0, R_t = 0, E_t = 0$ ) to obtain a four dimensional dynamical system. Traveling pulses represent homoclinic orbits about the unique fixed point. (Figure 3) The dispersion curve has a similar form to the well studied Fitzhugh-Nagumo model of excitability, in which the bottom of each curve represents an unstable wave, and the top represents a stable wave. We conjecture the same behaviour applies in our model. (Figure 4)

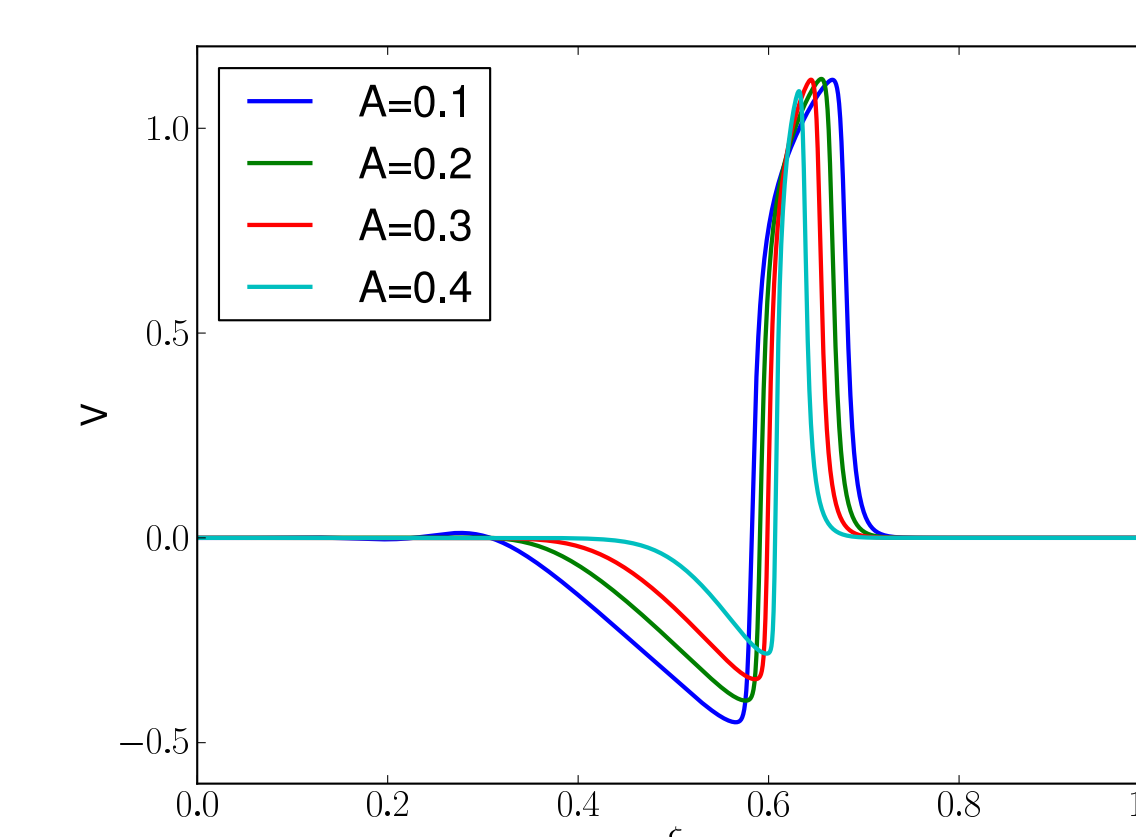


**Figure 3:** Form of traveling pulse for different values of  $A$ . Here  $\varepsilon = 0.1, B = 0.2, C = 0.2, \beta = 0.7, \gamma = 0.7, \kappa = 100, V_0 = 0.3$ . Computed in AUTO

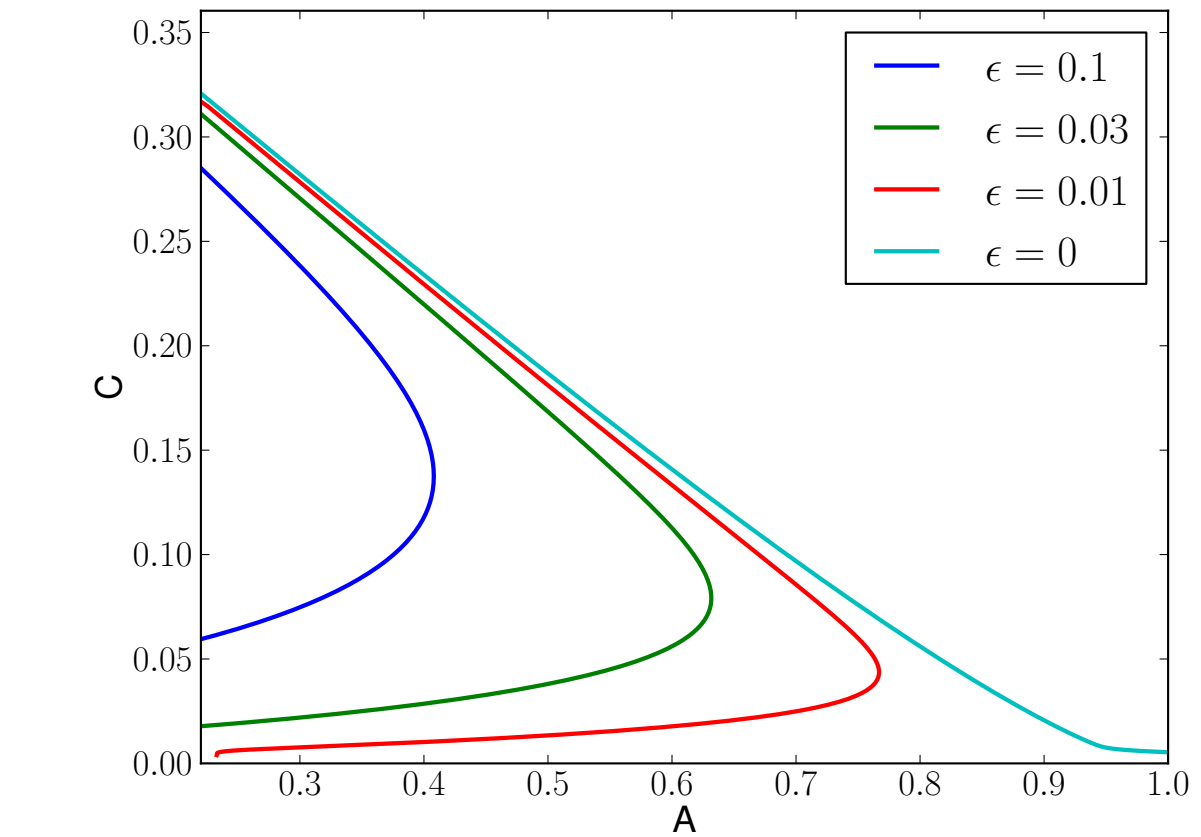


**Figure 4:** Wave speed as a function of parameter  $A$  for different values of  $\varepsilon$ . The  $\varepsilon = 0$  case is calculated from the singular perturbation analysis above. Computed in AUTO

## Stochastic models

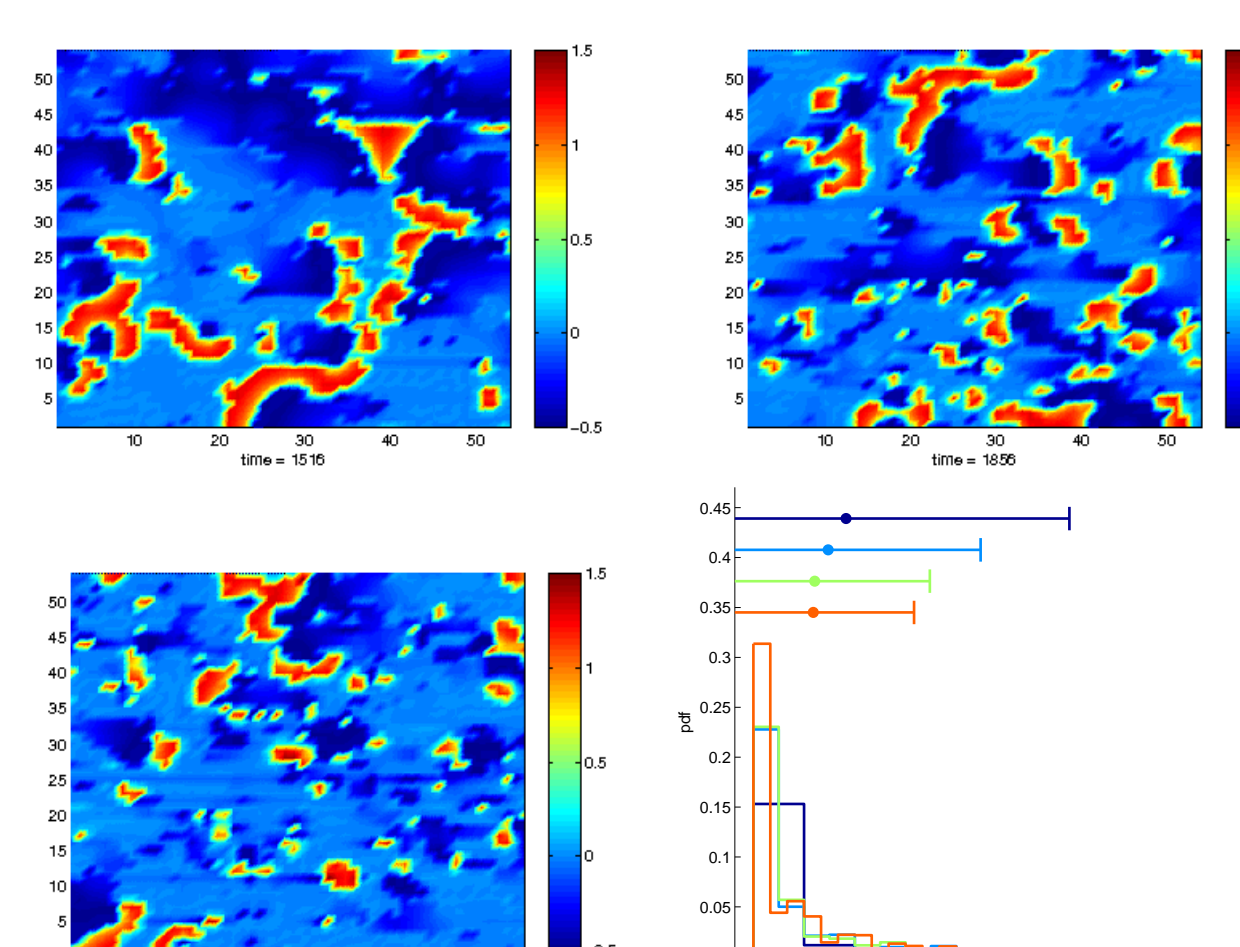


**Figure 5:** Simulations with noise. In order, left-right, top-bottom. Simulation for  $n = 1$ ; simulation for  $n = 2$ ; simulation for  $n = 3$ ; histogram of wave size distributions for  $n = 3$ . Bars show mean and IQR. Zoomed out spacings [3].

The size and duration of waves which form depends on the amount of noise which is added to simulations. At each time step  $n$  points on the grid are chosen and Gaussian noise is added to  $V$  and  $R$  variables. Without much noise large waves form which cover the entire domain and combine with other waves. With more noise smaller structures can form with wave size distributions more closely resembling power-law distributions observed *in vivo*. (Figure 5)

The Ford model [3] reports the same result by adding variability to the refractory time scale for each cell. This is produced here without assuming cell-cell variability is important. The per-cell spontaneous activation rate in our simulations is very low, consistent with physiological recordings [1, 2, 3, 4].

Figure 5 demonstrates too much wave activity – an effect which would be countered by the inclusion of a sAHP current.

## Conclusions and Future Work

We have developed a mathematical framework to study models of retinal waves. A mixture of asymptotic and continuation analysis allows for the computation of wave speed, wave duration and interwave-intervals as a function of model parameters. Simulations show type and amount of noise in system has large effect on wave structures. Analysis is to be repeated for more biophysically based model which includes a sAHP current, the stability of waves in one dimensional model is to be studied and the role noise plays in determining wave properties is to be more fully investigated.

## References

- [1] A. G. Blankenship and M. B. Feller, "Mechanisms underlying spontaneous patterned activity in developing neural circuits," *Nature reviews Neuroscience*, vol. 11, pp. 18–29, Jan. 2010.
- [2] J. Gjorgjieva and S. J. Eglen, "Modeling developmental patterns of spontaneous activity," *Current opinion in neurobiology*, vol. 21, pp. 679–84, Oct. 2011.
- [3] K. J. Ford, A. L. Félix, and M. B. Feller, "Cellular mechanisms underlying spatiotemporal features of cholinergic retinal waves," *The Journal of neuroscience : the official journal of the Society for Neuroscience*, vol. 32, pp. 850–63, Jan. 2012.
- [4] J. Keener and J. Sneyd, *Mathematical Physiology*. Springer, 2001.